Published online 30 March 2020

Nucleic Acids Research, 2020, Vol. 48, No. 9 ***e54***
doi: 10.1093/nar/gkaa181

Preferential production of RNA rings by T4 RNA ligase 2 without any splint through rational design of precursor strand

Hui Chen[1], Kai Cheng[1], Xiaoli Liu[1], Ran An[1,2,*], Makoto Komiyama[1] and Xingguo Liang[1,2,*]

[1]College of Food Science and Engineering, Ocean University of China, Qingdao 266003, China and [2]Laboratory for Marine Drugs and Bioproducts, Qingdao National Laboratory for Marine Science and Technology, Qingdao 266235, China

Received November 19, 2019; Revised February 04, 2020; Editorial Decision March 06, 2020; Accepted March 11, 2020

ABSTRACT

Rings of single-stranded RNA are promising for many practical applications, but the methods to prepare them in preparative scale have never been established. Previously, RNA circularization was achieved by T4 RNA ligase 2 (Rnl2, a dsRNA ligase) using splints, but the yield was low due to concurrent intermolecular polymerization. Here, various functional RNAs (siRNA, miRNA, ribozyme, etc.) are dominantly converted by Rnl2 to the rings without significant limitations in sizes and sequences. The key is to design a precursor RNA, which is highly activated for the efficient circularization without any splint. First, secondary structure of target RNA ring is simulated by Mfold, and then hypothetically cut at one site so that a few intramolecular base pairs are formed at the terminal. Simply by treating this RNA with Rnl2, the target ring was selectively and efficiently produced. Unexpectedly, circular RNA can be obtained in high yield (>90%), even when only 2 bp form in the 3′-OH side and no full match base pair forms in the 5′-phosphate side. Formation of polymeric by-products was further suppressed by diluting conventional Rnl2 buffer to abnormally low concentrations. Even at high-RNA concentrations (e.g. 50 μM), enormously high selectivity (>95%) was accomplished.

INTRODUCTION

Circular single-stranded RNAs (C-RNAs) are RNA rings without terminals, which are promising for many practical applications both *in vivo* and *in vitro*. Recently, for example, thousands of circular RNAs (circRNAs) have been found almost in all kingdom of organisms (1–5), and their biological roles as miRNA or RNA inhibitors have been reported (6–12). Many circRNAs have also been found to be translated or regulate functions of other proteins (6). Accordingly, artificial synthesis of C-RNAs has attracted much more interest for significant applications (13–15). One of the most advantageous properties of C-RNAs, which greatly facilitates their practical applications, is that they are strongly resistant against exo-ribonucleases, compared with non-cyclic linear RNAs (L-RNAs) (16–24). For example, siRNA effects of dumbbell-shaped C-RNAs were very high in living cells, primarily because of their long life-time (16–19). By combining the ring of antisense RNA strand with linear sense strand, off-target effects were reduced (20). Cyclic ribozymes (15) and cyclic RNA aptamers (21–23) were also developed to regulate their functions. Rolling circle translation of C-RNAs in cells was reported (25,26). Furthermore, circularization of L-RNAs is also useful to temporarily cage their intrinsic functions (e.g. ribozyme activity and gene-silencing) (18–20). By opening the rings with photo-irradiation or other outer stimuli, the latent functions were restored at desired place and timing (18,19). Valuable roles of C-RNAs in nanoarchitectures are also evident (27,28). All these results confirm enormously significant and promising features of C-RNAs for versatile applications. However, the information on their synthesis has been seriously insufficient, and there has been no way to prepare C-RNAs of desired sequences and sizes in preparative scale.

In most cases, C-RNAs are synthesized by circularizing L-RNAs with the use of enzymes. T4 RNA ligase 2 (T4 Rnl2) has been often used (13–15,29–32). The pioneering work by Yin *et al*. (29) showed that some L-RNAs were circularized by this enzyme to the rings. However, direct applications of this finding to preparation of various C-RNAs are not very successful, since the efficiency of circularization is highly dependent on the structure of L-RNA. Accordingly, in most cases, auxiliary oligonucleotide (called as splint), which is complementary with the terminal portions of L-RNA, was added to place the two ends close to each other (Scheme 1A) (26,31). The resultant nick structure is

*To whom correspondence should be addressed. Tel: +86 532 8203 1086; Fax: +86 532 8203 1086; Email: liangxg@ouc.edu.cn
Correspondence may also be addressed to Ran An. Tel: +86 532 8203 1318; Fax: +86 532 8203 1086; Email: ar@ouc.edu.cn

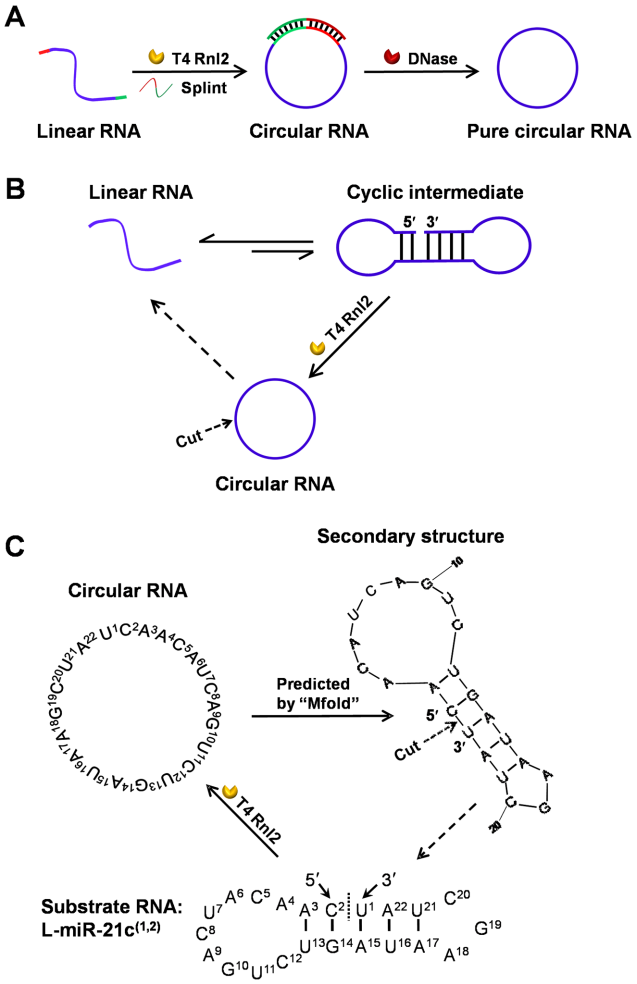

Scheme 1. Two strategies to circularize L-RNA to C-RNA by Rnl2. (**A**) Previous strategy using a splint, which is complementary with both the 3′-OH and 5′-phosphate ends of L-RNA. The splint has to be digested later by DNase or other nucleases. This method produces significant amounts of polymeric by-products, as shown in Figure 1. (**B**) The 'terminal base-pair strategy' in this study. On the basis of the secondary structure of C-RNA, C-RNA is hypothetically cut at a new site so that a few base pairs are formed near the ligation site. By treating the resultant L-RNA with Rnl2 (no splint is required), C-RNA is efficiently produced. Without the base-pair formation near the ligation site, Rnl2 hardly ligates the two ends to form C-RNA. (**C**) Scheme of C-RNA preparation using the substrate of L-miR-21c, the complementary sequence (inhibitor) of mircoRNA-21, as an example (41). The optimal substrate L-miR-21c$^{(1,2)}$ is obtained by hypothetically cutting the C-RNA between U^1 and C^2 on the basis of the predicted structure of C-miR-21c by Mfold (40).

recognized by Rnl2 (a dsRNA ligase). A similar methodology is being employed to prepare the rings of single-stranded DNA (32–34). It has been found that appropriate efficiency is favourable to suppress intermolecular ligation of ssDNA circularization (33,34). With this method, however, desired intramolecular RNA circularization is always accompanied by troublesome intermolecular polymerization of L-RNA, especially for higher RNA concentrations (Figure 1B). This concurrent polymerization notably lowers the yields of C-RNAs, and complicates the synthetic procedures. Furthermore, smaller-sized rings are hardly obtainable with this strategy, since cyclic intermediates involving short L-RNA (e.g. <30 nt) and splint are sterically unstable (33,34). Even with the use of T4 RNA ligase 1 (a single-stranded RNA specific ligase), intermolecular polymerization is dominant at high-substrate concentrations in many cases (13,26). In order to reduce the polymerization, specially designed DNA templates (helper) must be used (13,15). Circularization by ssRNA circligase™ (Epicentre Co.) requires Mn^{2+} as an essential cofactor, and relatively large amount of ligase is essential for high yield of ligation even at a low concentration of substrates (35–37).

We present here a facile and straightforward method to solve these problems on the basis of ligation mechanism of Rnl2. This enzyme binds to the 3′-OH side of a nick prior to the adenylation of the 5′-phosphate (37,38). We also found that even only small number of base pairs (≤4 bp) at ligation site greatly promote the ligation (39). Accordingly, we have here optimized the structures of L-RNA substrates for the circularization by Rnl2 through a rational design, so that a few base pairs are formed by the aid of Rnl2 at the ligation site. Note that all the L-RNAs formed by one-site scission of C-RNA at various positions yields the same C-RNA after circularization. Surprisingly, very efficient circularization can be accomplished, when only two base pairs are placed in the 3′-OH side. Without the use of any splint, a variety of functional L-RNAs (siRNA, miRNA and ribozymes) are circularized in high selectivity and yield. Formation of polymeric by-products is minimized even at high-substrate concentrations (e.g. >20 μM). Furthermore, the selectivity can be further promoted by using highly diluted Rnl2 buffer and elevating reaction temperature. By combining our findings, practical method to synthesize C-RNAs in preparative scale and high selectivity has been developed.

Outline of the present 'terminal base-pair strategy' for dominant preparation of C-RNA

The present strategy is schematically depicted in Scheme 1B and C. The key point is the design of L-RNA substrate with appropriate reactivity for T4 Rnl2 ligation, which is efficient enough for intramolecular circularization but not reactive for intermolecular ligation. First, the secondary structure of target C-RNA is determined by Mfold prediction (40,41). Then, the ring is hypothetically cut at one position to give the optimal L-RNA substrate. The optimal substrate is chosen from a pool of L-RNAs obtained by the hypothetical scission of the desired C-RNA. The criterion of choice is the numbers of base pairs formed in the 3′-OH side and the 5′-phosphate side of the ligation site. Wobble base pairs are acceptable. As shown later, 2 bp in the 3′-OH side of joining site is enough for circularization, and additional one base pair in the 5′-phosphate side can further accelerate the circularization. It should be noted that these base pairs for L-RNA substrate are allowed to be unstable in the absence of Rnl2. In the presence of Rnl2, however, the strong binding of Rnl2 can stabilize the nick structure (39). Most RNAs can take notable secondary structures (>3 continuous base pairs), and thus the optimal L-RNA is in almost all the cases easily designable.

The determined optimal L-RNA is prepared by a synthesizer, and finally treated with T4 Rnl2 in the absence of any splint. By this simple method, target C-RNA is se-

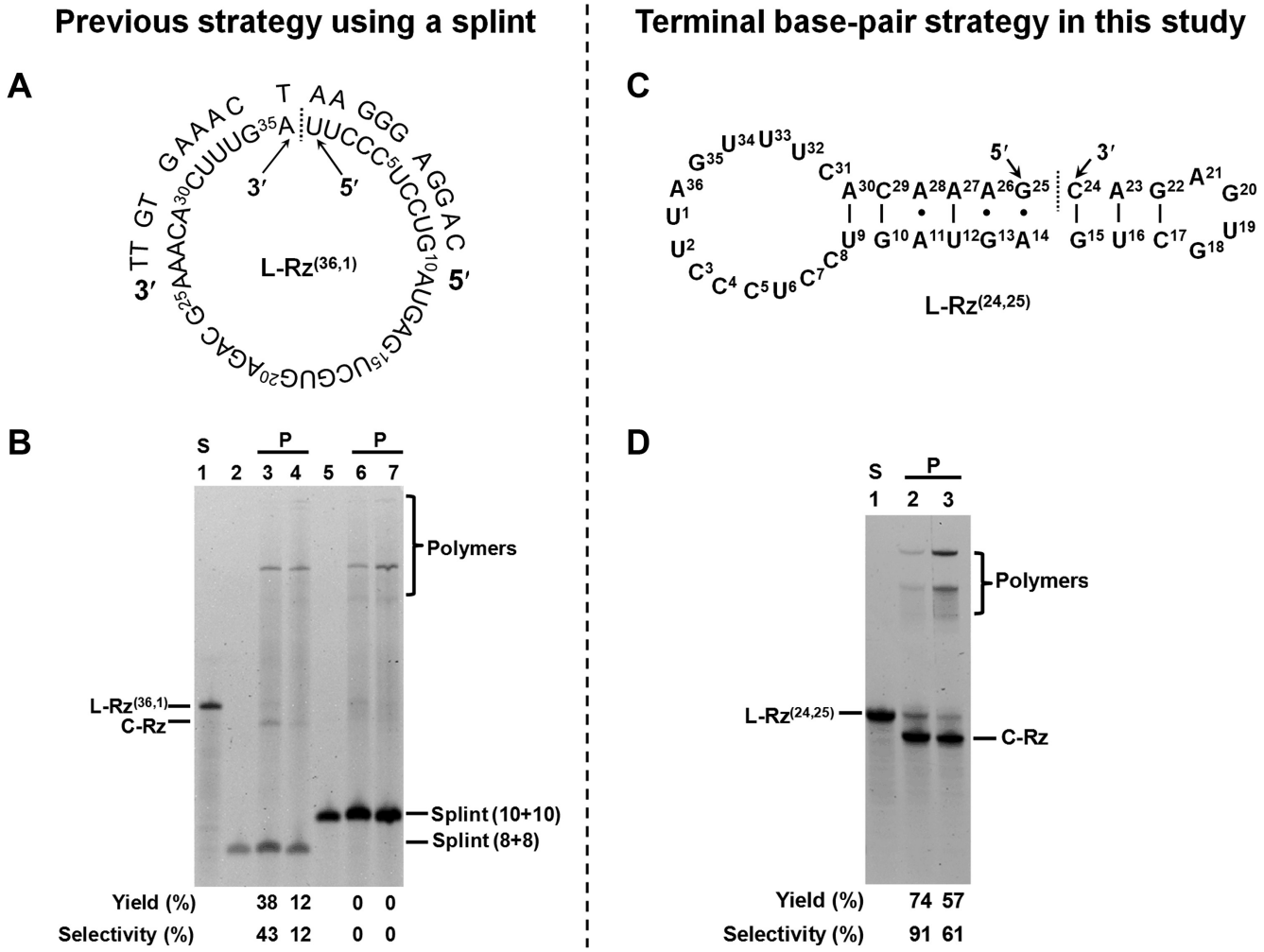

Figure 1. Preparation of the ring of c-erbB-2-specific hammerhead ribozyme by Rnl2 through either the conventional (**A** and **B**) or present strategy (**C** and **D**). (A) Structure of conjugate between the original c-erB-2 hammerhead ribozyme (L-Rz$^{(36,1)}$) and 20-nt splint. The ligation site by Rnl2 is shown by dotted line. (B) 12% dPAGE analysis of the ligation products (P) using the original strategy. Lane 2, 16-nt splint; Lanes 3 and 6, $[\text{L-RNA}]_0 = 2$ μM; Lane 5, 20-nt splint; Lanes 4 and 7, $[\text{L-RNA}]_0 = 10$ μM. Here, 'S' refers to linear RNA (L-RNA). (C) Structure of precursor L-RNA (L-Rz$^{(24,25)}$) used for the present strategy. According to the prediction by Mfold, C-Rz was cut between C^{24} and G^{25}. (D) About 12% dPAGE analysis of the ligation products using the present strategy. Lane 2, $[\text{L-RNA}]_0 = 2$ μM; Lane 3, $[\text{L-RNA}]_0 = 10$ μM. Circularization conditions: [T4 Rnl2] = 0.2 U/μL, 1 × T4 Rnl2 buffer, [splint] / [L-RNA] = 2, 25°C. The reaction time is 2 h for $[\text{L-RNA}]_0 = 2$ μM, and 6 h for $[\text{L-RNA}]_0 = 10$ μM, respectively.

lectively obtained in high yields, with minimal production of polymeric by-products. No complicated purification of the products is necessary, because no additional oligonucleotides are present.

MATERIALS AND METHODS

Materials

All oligoRNAs used in this study were synthesized by GENEWIZ, Inc. (Suzhou, China), and the sequences are listed in Supplementary Table S1. For ligation experiments, a phosphate was in advance introduced to the 5′-position of L-RNA by using T4 polynucleotide kinase (Thermo Scientific; Pittsburgh, PA, USA). RiboLock RNase Inhibitor was also from Thermo Scientific. Ultra GelRed was from Vazyme (Nanjing, China). T4 Rnl2 and Exonuclease T were purchased from NEW ENGLAND BioLabs (Beijing, China). All other chemicals were from Sigma-Aldrich (St. Louis, MO, USA).

Circularization of L-RNA by T4 Rnl2

Reactions in 1 × T4 Rnl2 buffer. A typical mixture (10 μl) was composed of 1 μM L-RNA, 2 U Rnl2 and 20 U RiboLock RNase Inhibitor in 1 × T4 Rnl2 buffer (50 mM Tris–HCl (pH 7.5), 2 mM $MgCl_2$, 1 mM DL-Dithiothreitol (DTT) and 400 μM adenosine triphosphate (ATP)). We pre-treated RNA samples at 80°C for 3 min, and cooled to the reaction temperature at a rate of 6°C/min. Then, the reaction was carried out at 25°C for 2 h (unless noted otherwise), and terminated by heating the mixture at 75°C for 10 min (details are presented in Supplementary Materials). The cyclic structures of reaction products were confirmed by treating them with Exonuclease T (5 U) at 25°C for 6 h.

Reactions in diluted Rnl2 buffers. The commercially obtained T4 Rnl2 ligase buffer was diluted by water, and used for the ligation. Otherwise, all the procedures were exactly the same as described above.

Prediction of the secondary structures of RNAs by Mfold

The secondary structures of C-RNAs and L-RNAs were predicted at [NaCl] = 1.0 M and 37°C by the Mfold Web Server using 'RNA Folding Form (version 2.3 energies)'. The website: http://unafold.rna.albany.edu/?q=mfold/RNA-Folding-Form2.3 (40).

Evaluation of the yield and selectivity for the formation of RNA rings

After the enzymatic reactions, the products were diluted and subjected to the electrophoresis with 12% denaturing polyacrylamide gel containing 8 M urea (dPAGE), stained by Ultra GelRed, and then imaged with a UV Gel imager from BIO-RAD (Hercules, USA). Quantitative data were obtained by using Image Lab software. The yield and selectivity for the formation of RNA rings were calculated by the following equations:

$$\text{Yield}(\%) = \frac{C}{S+P} \times 100$$

$$\text{Selectivity}(\%) = \frac{C}{P} \times 100$$

Here, C, S and P were the band intensities of the circular RNA (C-RNA) to be synthesized, linear substrate RNA (L-RNA) and all products derived from L-RNA (consisting of C-RNA, AppRNA (adenylated intermediate) and polymeric by-products), respectively. Each experiment has been repeated at least three times, and the quantitative error of band brightness was within 10%.

RESULTS

In the present methodology, a few base pairs were intentionally placed at the ligation site of precursor L-RNAs to promote the circularization by T4 Rnl2. The numbers of base pairs, as well as the reaction conditions, were systematically changed to optimize the yield and the selectivity. Cyclic structures of the ring products were confirmed by their complete resistance against Exonuclease T. It is noteworthy that all the L-RNAs used here have biological and other important functions (siRNA, miRNA, ribozyme and others).

Improved efficiency of the present 'terminal base-pair strategy' compared to 'conventional (template-mediated) strategy'

In Figure 1, c-erbB-2-specific hammerhead ribozyme was treated by Rnl2 through the two strategies (42). Its circular form has been shown to have much less activity (43). In Figure 1A and B (conventional template-mediated strategy), the original ribozyme (L-Rz$^{(36,1)}$) was directly employed as the substrate for the enzymatic circularization (its detailed structure for RNA cleavage is presented in Supplementary Figure S1). In the presence of a splint (either 16- or 20-nt), L-Rz$^{(36,1)}$ was mostly converted to polymeric by-products (Figure 1B). With the use of 20-nt splint, for example, almost no desired circularization product (C-Rz) was obtained (lanes 6 (2 μM) and 7 (10 μM) in Figure 1B). With 16-nt splint, some amounts of C-Rz were produced, but the selectivity values were only 43 and 12% when 2 and 10 μM of L-Rz$^{(36,1)}$ were used, respectively (lanes 3 and 4). All the attempts to improve the efficiency by optimizing the reaction conditions, such as temperatures (37°C and 45°C), buffer concentrations (0.5 × and 0.1 ×), splint lengths (> 12 nt) and substrate adding method (changed from 'one-pot' to 'step by step'), were not successful. It was concluded that conventional template-mediated method is hard to provide C-RNA efficiently.

To solve above problems, 'terminal base-pair strategy' was employed as shown in Figure 1C and D. The conformation of C-Rz was first predicted by Mfold, and L-RNA precursor was designed by hypothetically cutting C-Rz between C^{24} and G^{25}. In the resultant RNA (L-Rz$^{(24,25)}$ in Figure 1C), three Watson-Crick base pairs are formed in the 3′-OH side of the ligation site. On the other hand, there exists no stable Watson–Crick pairs in the 5′-phosphate side (only the third, fifth and sixth pairs are matching). It has been reported that consecutive non-Watson–Crick pairs can form, stabilizing the coaxial stacking with 3′-OH side duplex (44,45). Figure 1D shows the ligation result of L-Rz$^{(24,25)}$ by Rnl2 without using a splint. As shown in lanes 2 and 3, targeted C-Rz was efficiently produced (the strong bands at the bottom). The selectivity for the formation of C-Rz was 91% at [L-Rz$^{(24,25)}$] = 2 μM (lane 2). Even when [L-Rz$^{(24,25)}$] was increased to 10 μM, this new strategy provided C-Rz in 61% selectivity (lane 3). These values are much higher than those for the template-mediated strategy shown in Figure 1B. As Rnl2 has been considered as an enzyme to ligate nicks for a long time, it is surprising that efficient ligation occurred with only 3 bp formed at 3′-OH side.

When L-Rz$^{(36,1)}$ was circularized in the absence of any splint (Supplementary Figure S12), the circularization yield was as high as 75% after 2 h (nearly the same as that of L-Rz$^{(24,25)}$). Surprisingly, no intermolecular polymeric byproducts were found and the selectivity for C-Rz was 100%, which is even better than that of L-Rz$^{(24,25)}$ (selectivity = 91% in lane 2 of Figure 1D). The possible secondary structures of L-Rz$^{(36,1)}$ (depicted in Supplementary Figure S12A) may improve the circularization efficiency.

Even with our new strategy, polymeric by-products were also produced to some extent, especially at higher concentrations (lane 3 in Figure 1D). However, this problem is successfully solved by optimizing the reaction conditions, leading to still more effective preparation method (see below).

Applicability of 'terminal base-pair strategy' to circularization of versatile L-RNAs by T4 Rnl2

At first, two kinds of 21-nt L-RNAs were treated by T4 Rnl2 at 25°C (Figure 2). Both L-RNAs are precursors of the ring of GAS-siRNA (C-siR-GAS) which suppresses the expression of GFP gene (20), and have several base pairs at the ligation site. It is noteworthy that, for both of these

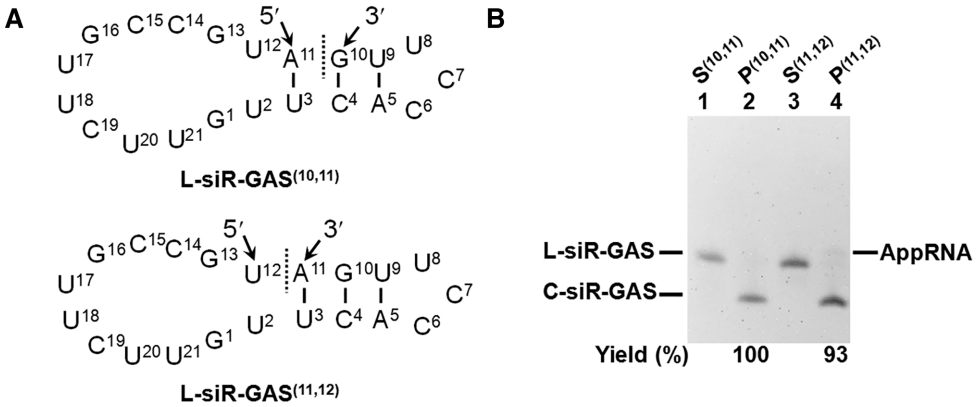

Figure 2. Predominant role of terminal base pairs on the preparation of C-siR-GAS by T4 Rnl2. (**A**) Proposed structures of L-siR-GAS$^{(10,11)}$ and L-siR-GAS$^{(11,12)}$. The ligation sites by Rnl2 are shown by dotted lines. These two precursors are formed by hypothetically cutting C-siR-GAS. For example, L-siR-GAS$^{(10,11)}$ is formed by the scission between G^{10} and A^{11}. (**B**) Ligation of these L-RNAs by Rnl2. Lane 1, L-siR-GAS$^{(10,11)}$ only; lane 2, treatment of L-siR-GAS$^{(10,11)}$ with Rnl2; lane 3, L-siR-GAS$^{(11,12)}$ only; lane 4, treatment of L-siR-GAS$^{(11,12)}$ with Rnl2. Circularization conditions: [L-RNA] = 2 μM, [T4 Rnl2] = 0.2 U/μl, 1 × T4 Rnl2 buffer, 25°C, 2 h.

two precursors, the circularization proceeded with remarkable efficiency. In contrast with the splint-assisted ligation in Figure 1, almost no polymeric by-products were produced. The selectivity for the circularization was virtually 100%. For example, L-siR-GAS$^{(11,12)}$ (the lower sequence in Figure 2A) is obtained by hypothetically cutting C-siR-GAS between A^{11} and U^{12}. Three Watson–Crick pairs (A^{11}-U^3, G^{10}-C^4 and U^9-A^5) are formed in the 3′-OH side of the ligation site, whereas no base pair exists in the 5′-phosphate side. Upon the treatment by Rnl2, this L-RNA was rapidly and selectively converted to C-siR-GAS, and the yield was 93% after only 2 h (lane 4). Almost no adenylated L-RNA was accummulated, since this intermediate of enzymatic reaction is rapidly converted to the final product. The production of C-siR-GAS was still more efficient, when the cutting site of C-siR-GAS was shifted by one base toward 3′-OH side to form the precursor L-siR-GAS$^{(10,11)}$ with 2 bp in the 3′-OH side and 1 bp in the 5′-phosphate side (the upper sequence in Figure 2A). This precursor was far more reactive than L-siR-GAS$^{(11,12)}$ (*vide infra*), and almost quantitatively converted to C-siR-GAS only in 2 h (lane 2).

The ring of siRNA Eg5 (C-siR-Eg5), which allows tumour cells to stay in the G2 phase (46), was also successfully prepared (lanes 2 of Supplementary Figure S2B and C). In L-siR-Eg5$^{(12,13)}$, 3 bp are formed in the 3′-OH side, and an A-T pair and a wobble G-U pair are formed in the 5′-phosphate side. No polymeric by-products were perceived in the gel, and the selectivity for the ring was almost 100% at [L-siR-Eg5$^{(12,13)}$] = 2 μM (Supplementary Figure S2B). These two results show that concurrent polymerization can be sufficiently suppressed when there exist only 2 or 3 bp in the 3′-OH side of the ligation site.

Effects of the numbers of terminal base pairs

As shown by the time-courses in Figure 3, L-siR-GAS$^{(10,11)}$ (in Figure 2A) was circularized by Rnl2 much faster than L-siR-GAS$^{(11,12)}$ (see original data in Supplementary Figure S3). When [L-siR-GAS$^{(10,11)}$] = 1 μM and [Rnl2] = 0.2 U/μl, more than 50% of the substrate was circularzed in 10 min to C-siR-GAS (Figure 3A). Even at the substrate concentration of 10 μM ([Rnl2] = 1 U/μl), the yield of ring was 49% at 10 min (Figure 3B). The corresponding values for L-siR-GAS$^{(11,12)}$ were 10% at 1 μM and 5% at 10 μM. Apparently, 2 bp in the 3′-OH side (and 1 bp in the 5′-phosphate side) for L-siR-GAS$^{(10,11)}$ are more favorable for the intramolecular circularization than 3 bp in the 3′-OH side (and none in the 5′-phosphate side) for L-siR-GAS$^{(11,12)}$. In another way to say, the ligation is greatly increased by the presence of only 1 bp in the 5′-phosphate side, although such a short base pair is usually hard to form without the help of Rnl2. Similar time-courses were obtained under other conditions (Supplementary Figure S4).

During comprehensive studies, we found that several base pairs are often consecutively formed in many C-RNAs. For example, C-miR-21c, which is complementary to endogenous miRNA 21 (miR-21) and used as its inhibitor (41), involves five consecutive base pairs. Accordingly, to analyze the effects of the numbers of base pairs in both sides of the ligation site, the position of hypothetical cutting of the ring was systematically shifted in Figure 4. Upon the treatment with Rnl2, all these precursors efficiently provided C-miR-21c. However, the polymeric by-products were not negligible for the circularization of these substrates (upper part of the gel). The contribution of concurrent polymerization drastically increased with increasing number of base pairs in the 5′-phosphate side. Thus, L-miR-21c$^{(22,1)}$ (3 bp in the 5′-phosphate side of the ligation site) was mostly converted to the polymers, and only minimal amount of C-miR-21c was obtained (lane 8, Figure 4). On the other hand, the selectivity for the circularization increased to around 60% for L-miR-21c$^{(1,2)}$ (2 bp in the 5′-phosphate side; lane 6). With the precursors having 0 or 1 bp in the 5′-phosphate side (L-miR-21c$^{(3,4)}$ and L-miR-21c$^{(2,3)}$), the formation of polymeric by-products was minimized. Apparently, too many base pairs in the 5′-phosphate side are unfavorable to suppress the intermolecular ligation by Rnl2.

From the results in Figures 1–3, it can be concluded that the base pairs in the 3′-OH side should be two or larger.

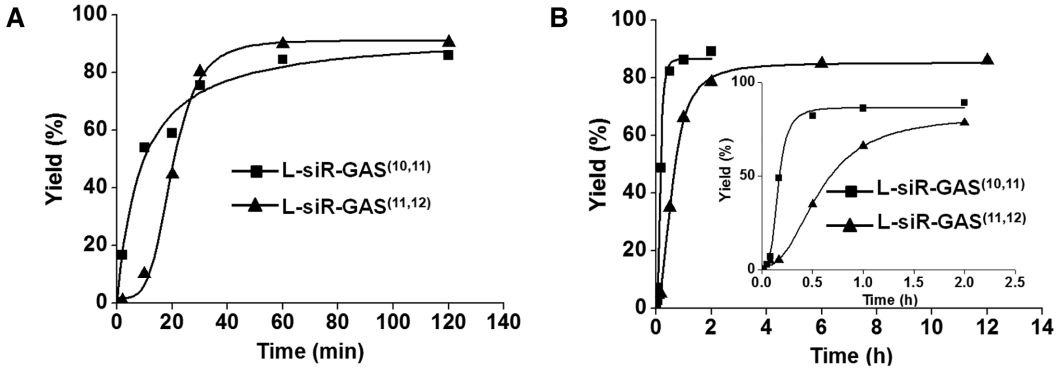

Figure 3. Time-courses for the circularization of L-siR-GAS$^{(10,11)}$ and L-siR-GAS$^{(11,12)}$ by Rnl2 at 25°C. (**A**) [L-RNA] = 1 μM and [Rnl2] = 0.2 U/μl. (**B**) [L-RNA] = 10 μM and [Rnl2] = 1 U/μl.

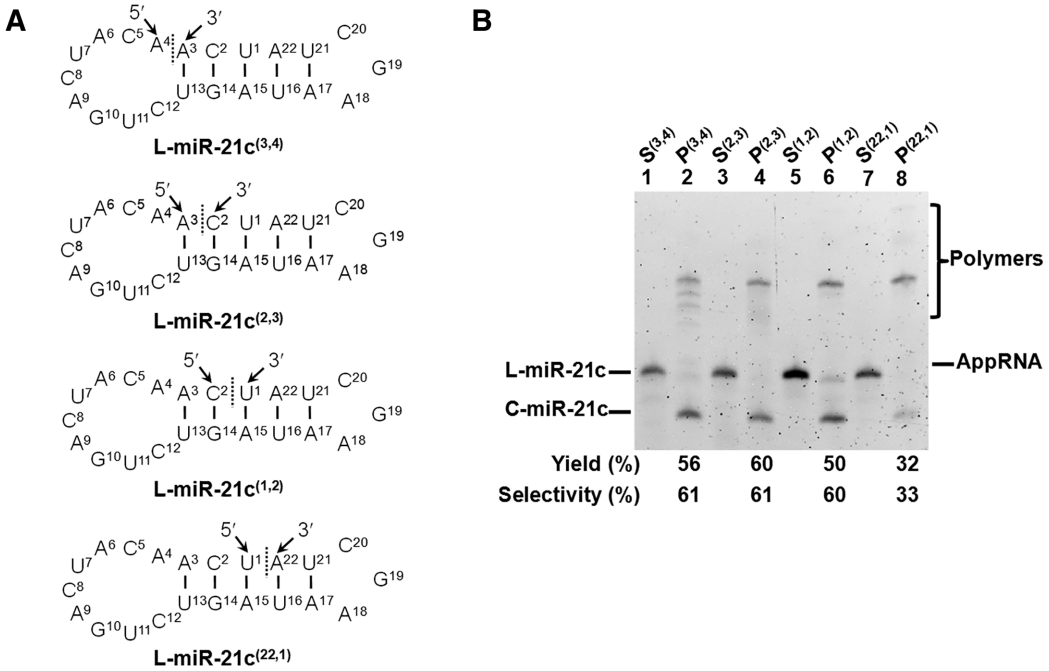

Figure 4. Effects of the numbers of terminal base pairs on the circularization efficiency by T4 Rnl2. (**A**) Proposed structures of L-miR-21c$^{(3,4)}$, L-miR-21c$^{(2,3)}$, L-miR-21c$^{(1,2)}$ and L-miR-21c$^{(22,1)}$. The numbers of base pairs in the 3′-OH and 5′-phosphate sides of ligation site are (5,0), (4,1), (3,2) and (2,3), respectively. (**B**) 12% dPAGE for the cyclization products. Conditions: [L-RNA] = 10 μM, [T4 Rnl2] = 1 U/μl, 1 × T4 Rnl2 buffer, 25°C, 12 h.

On the other hand, the base pairs in the 5′-phosphate side should be kept 0 or 1, since further increase in the number deteriorates the selectivity. Too many base pairs (e.g. ≥4 bp) at 3′-OH side may also increase polymeric by-products (implicated by the results depicted in Supplementary Figure S2B and C). For L-siR-GAS-A$^{(11,12)}$, in which 4 bp form in the 3′-OH side, and two G-U wobble pairs form in the 5′-phosphate side, more polymers were produced as compared with L-siR-GAS$^{(11,12)}$ (compare lanes 4 in Supplementary Figure S2 with lane 4 of Figure 2). It is noteworthy that even only 1 bp in the 3′-OH side is also acceptable, since it simply decreases the reaction rate (see the 'Discussion' section). Interestingly, the intermolecular ligation can be completely suppressed by the formation of less base pairs in the 3′-OH side, although longer reaction time may be required to give high yield of C-RNA (as shown later).

Optimization of reaction conditions for further promotion of the efficiency

In order to accomplish still higher efficiency by suppressing the polymeric by-products, the reaction conditions were optimized using L-miR-21c$^{(2,3)}$ as substrate.

Dilution of T4 Rnl2 buffer to suppress concurrent polymerization. The selectivity for C-miR-21c formation was drastically promoted, when the concentration of T4 Rnl2 buffer was decreased (Figure 5A). In commercially available 1 × T4 Rnl2 buffer, considerable amounts of polymeric by-products were concurrently produced, and thus the selectivity for the intramolecular circularization to the ring was about 57% (lane 2). In 0.1 × T4 Rnl2 buffer, however, the selectivity increased to 89% (lane 6). Assumedly, the in-

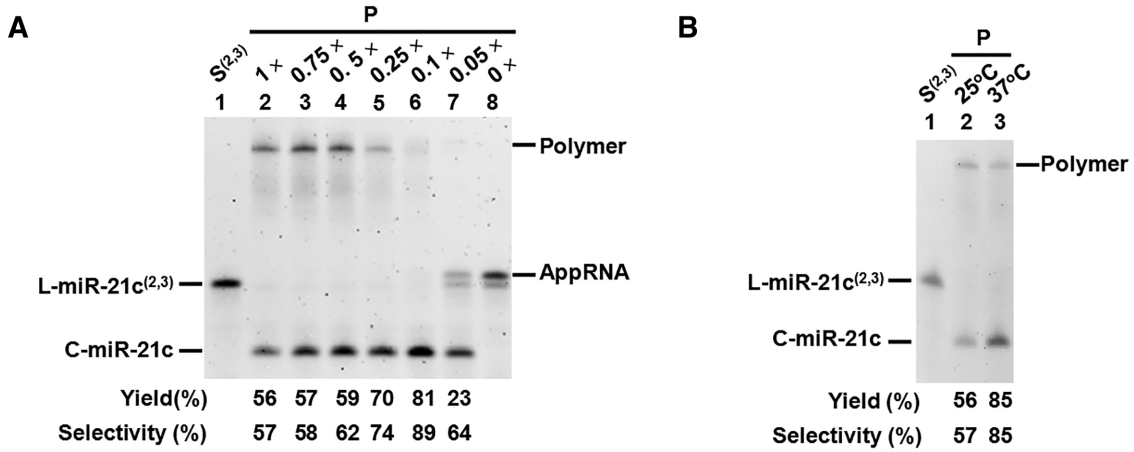

Figure 5. Effects of (**A**) concentration of T4 Rnl2 buffer and (**B**) reaction temperature on the efficiency of circularization of L-miR-21c$^{(2,3)}$. In (A), [L-RNA] = 10 μM, [T4 Rnl2] = 1 U/μl, 25°C, 12 h. In (B), [L-RNA] = 10 μM, [Rnl2] = 1 U/μl, 1 × Rnl2 buffer, 25°C or 37°C, 12 h. Note that 1 × ligase buffer contains 2 mM $MgCl_2$, 400 μM ATP, 50 mM Tris–HCl (pH 7.5) and 1 mM DTT.

termolecular ligation to polymeric by-products was suppressed in these diluted buffers, since lower Mg^{2+} concentrations enhanced the electrostatic repulsion between L-RNA molecules. Similar suppression of intermolecular polymerization by diluted ligase buffers was previously found in the production of single-stranded DNA rings from linear DNAs by T4 DNA ligase (33,34).

When the buffer concentration was too low (0.05 × buffer), the selectivity decresed to 64% due to the accumulation of notable amounts of adenylated L-miR-21c$^{(2,3)}$ as the reaction intermediate (lane 7). In addition, the enzymatic ligation was very slow, and some of L-miR-21c$^{(2,3)}$ was left unchanged even after 12 h of reaction (see also Supplementary Figure S6). In order to fulfill both high selectivity and satisfactorily high yield for C-RNA, the most appropriate concentration of T4 Rnl2 buffer is around 0.1×. Similar results were also obtained by using diluted buffers for L-miR-21c$^{(1,2)}$ and L-miR-21c$^{(22,1)}$ (Supplementary Figure S5). Compared with the reaction in 1 × T4 Rnl2 buffer, the rate in 0.1 × buffer was considerably smaller (Supplementary Figure S6). However, the reactions were completed within 10 h, and sufficiently fast for most of practical purposes.

Temperature effects. When the L-miR-21c$^{(2,3)}$ was treated by T4 Rnl2 at 37°C for 12 h, the targeted ring was produced in 85% selectivity (lane 3 of Figure 5B). This selectivity was considerably higher than that (57%) for the reaction at 25°C (lane 2). This remarkable temperature effect is ascribed to the decrease of intermolecular hybridization between two L-RNA molecules upon the increase of temperature from 25°C to 37°C. On the other hand, the intramolecular secondary structure of L-RNA is sufficiently stable to be bound by Rnl2 even at 37°C, and proceeds to the intramolecular circularization as we design.

Preparative-scale synthesis of target RNA rings by combining 'terminal base-pair strategy' with 'low-buffer concentration' and 'high temperature'

In Figures 6 and 7, 'terminal base-pair strategy' was accomplished in 0.1 × T4 Rnl2 buffer at 37°C, and C-RNAs

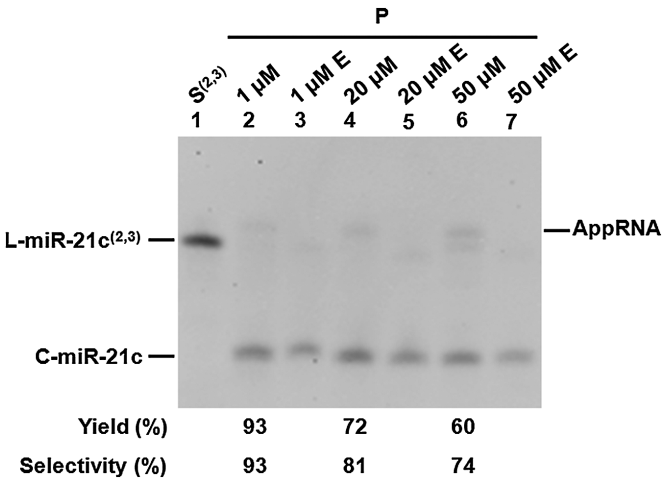

Figure 6. Highly selective preparative-scale circularization of L-miR-21c$^{(2,3)}$ by employing 'terminal base-pair strategy' in 0.1 × T4 Rnl2 buffer at 37°C. Lane 1, L-miR-21c$^{(2,3)}$ only; lane 2, [L-RNA] = 1 μM, [Rnl2] = 0.2 U/μl; lane 4, [L-RNA] = 20 μM, [Rnl2] = 2 U/μl; lane 6, [L-RNA] = 50 μM, [Rnl2] = 2 U/μl. [ATP (supplied by 0.1 × Rnl2 buffer)] = 40 μM. The reaction time was 12 h. In Ianes 3, 5 and 7, the products in lanes 2, 4 and 6 were treated with Exonuclease T.

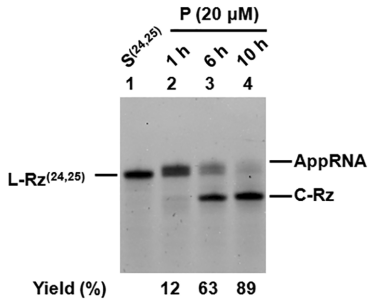

Figure 7. Highly selective preparative-scale circularization of L-Rz$^{(24,25)}$. Lane 1, L-Rz$^{(24,25)}$ only; lanes 2–4, circularization by Rnl2 for 1, 6 and 10 h. Reaction conditions: [L-RNA] = 20 μM, [T4 Rnl2] = 2 U/μl, [ATP] = 400 μM, 0.1 × Rnl2 buffer ([Mg^{2+}] = 200 μM), 37°C.

were selectively synthesized in a preparative scale. In Figure 6, the concentration of L-miR-21c$^{(2,3)}$ was increased to 20 and 50 μM, and the amount of Rnl2 was also increased from 0.2 to 2 U/μl. Even when the concentration of L-miR-21c$^{(2,3)}$ was 50 μM (the largest value investigated), the selectivity for the circularization was as high as 74% (lane 6) and the purity was almost 100% after digestion of linear RNA molecules (unreacted L-miR-21c$^{(2,3)}$ and its adenylated product) with Exonuclease T (lane 7). Formation of polymeric by-products, observed in 1 × Rnl2 buffer (lane 4 in Figure 4B), was completely inhibited. The yield was further increased about 10% by increasing [ATP] (Supplementary Figure S7).

The optimal conditions for the synthesis of C-miR-21c, determined by vigorous systematic studies, were as follows (Supplementary Figure S8). In 0.15 × buffer, the concentration of ATP was adjusted to 200 μM ([L-miR-21c$^{(2,3)}$] = 50 μM, [$MgCl_2$] = 300 μM and [T4 Rnl2] = 2 U/μl). After 32 h at 37°C, C-miR-21c was obtained in 97% selectivity and 85% yield. These values correspond to the production of about 30 mg of C-miR-21c from 100 ml of reaction mixture. The product is sufficiently pure for most of the applications. When necessary, further purification can also be carried out simply by Exonuclease T treatment. Further increase of [ATP] was not very successful, probably because of the interaction between ATP and Mg^{2+} (Supplementary Figure S9) (34,47–49).

Preparative-scale preparation of C-Rz was also successful by ligation at 37°C using 0.1 × T4 Rnl2 buffer (Figure 7). The yield from 20 μM of L-Rz$^{(24,25)}$ was almost 90%. The polymeric by-products were never produced even for a prolonged reaction (data not shown). This is a great improvement as compared with Figure 1D, in which 1 × T4 Rnl2 buffer was used at 25°C. About 21 mg of C-Rz are obtainable from 100 ml (20 μM) of reaction mixture. Compared with conventional splint-mediated method involving notable concurrent polymerization (Figure 1A), superiority of the present method is more conclusive.

DISCUSSION

'Terminal base-pair strategy' as an efficient method to prepare ssRNA rings in preparative scale

During RNA circularization, co-occurrence of intermolecular ligation to give troublesome polymeric byproducts has puzzled us for a long time. This problem is really difficult to solve because any change of reaction condition affects both intermolecular and intramolecular reactions. Fortunately, we found that target RNA ring can be obtained in high yield and selectivity through rational design of linear RNA precursor (L-RNA). There is no obvious limitation in the sequence and ring size. When the desired circular RNA is hypothetically cut at one position, the most appropriate L-RNA substrate can be designed by comparing the secondary structures of these substrate candidates. Unexpectedly, we found that the design is so easy to be realized, because it only requires 2–3 bp in the 3′-OH side at the ligation site, and even the absence of base pair in the 5′-phosphate side is acceptable (Figures 2 and 3). More interestingly, the intermolecular ligation can be almost completely suppressed by decreasing the number of base pairs in the 5′-phosphate side to 1 or 0. As a result, the desired circular RNA can be obtained in nearly 100% selectivity. The reaction is sufficiently fast enough to finish in several hours. This highly selective circularization is ascribed to the enlargement of the rate difference between intramolecular ligation and intermolecular ligation by the design of L-RNA precursor. The high selectivity is mainly attributed to the efficient suppression of intermolecular polymerization.

These results are fairly interpretable in terms of the reported characteristics and the mechanism of Rnl2. The activity of Rnl2 is pretty high, as compared with other ligases, probably due to its availability to the repair of many kinds of RNA damage *in vivo*. Accordingly, several base pairs at ligation site are enough to give efficient ligation, as we previously reported (39). The base pairs in the 3′-OH side at ligation site are absolutely essential for the present circularization, since they provide the binding site of Rnl2 to precursor L-RNA. During the closure of a nick in RNA duplex by Rnl2, the enzyme predominantly contacts with the 3′-OH side of the nick, as concretely evidenced by Nandakumar *et al*. (37). Then, the adenylated Rnl2 transfers the adenylyl group to the 5′-phosphate. At last, the adenylated phosphate is attacked by the 3′-OH to complete the formation of phosphodiester linkage (38,39). On the other hand, the base pairing in the 5′-phosphate side serves to minimize structural perturbation of the transition state for the circularization. As the result, the intramolecular ligation is greatly accelerated by these two kinds of base pairs. It is noteworthy that the pairings of such small number of consecutive base pairs successfully occur only intramolecularly, since they are promoted by less entropy loss as well as by binding affinity of Rnl2 (see the next section). In contrast, these base pairs can be only weakly formed between two L-RNA molecules. Thus, intermolecular polymerization is almost completely suppressed throughout the present study, and nearly 100% selectivity for C-RNA is accomplished. Consistently, the intermolecular ligation notably increases as the numbers of consecutive base pairs in both sides increase (Figures 1C and D, and 4). This side-reaction is more obvious, when the ligation is too fast (Supplementary Figure S10) (33,34). The formation of polymeric by-products is avoidable by using the conditions under which only intramolecular ligation occurs. Probably, the relatively favourable formation of intramolecular secondary structure as compared with intermolecular one can be strengthened when the ligation conditions are weak enough (or appropriate).

Since most RNAs fold to stable secondary structures, appropriate L-RNA precursor is easily obtainable. In many cases, almost 100% selectivity is easily accomplished only with 'terminal base-pair strategy'. For the other cases, in which this technology alone is insufficient for dominant production of RNA rings, simultaneous use of both 'low buffer concentration strategy' (Figure 5A) and 'higher reaction temperatures' (Figure 5B) are effective. By combining these three factors, highly pure circularization can be easily accomplished and desired RNA ring is obtained in a large scale (Figures 6 and 7; Supplementary Figure S8). Another merit of our apporach is that we can make different designs according to different requirements. If low concentration of substrate is acceptable, we can design and use the substrate

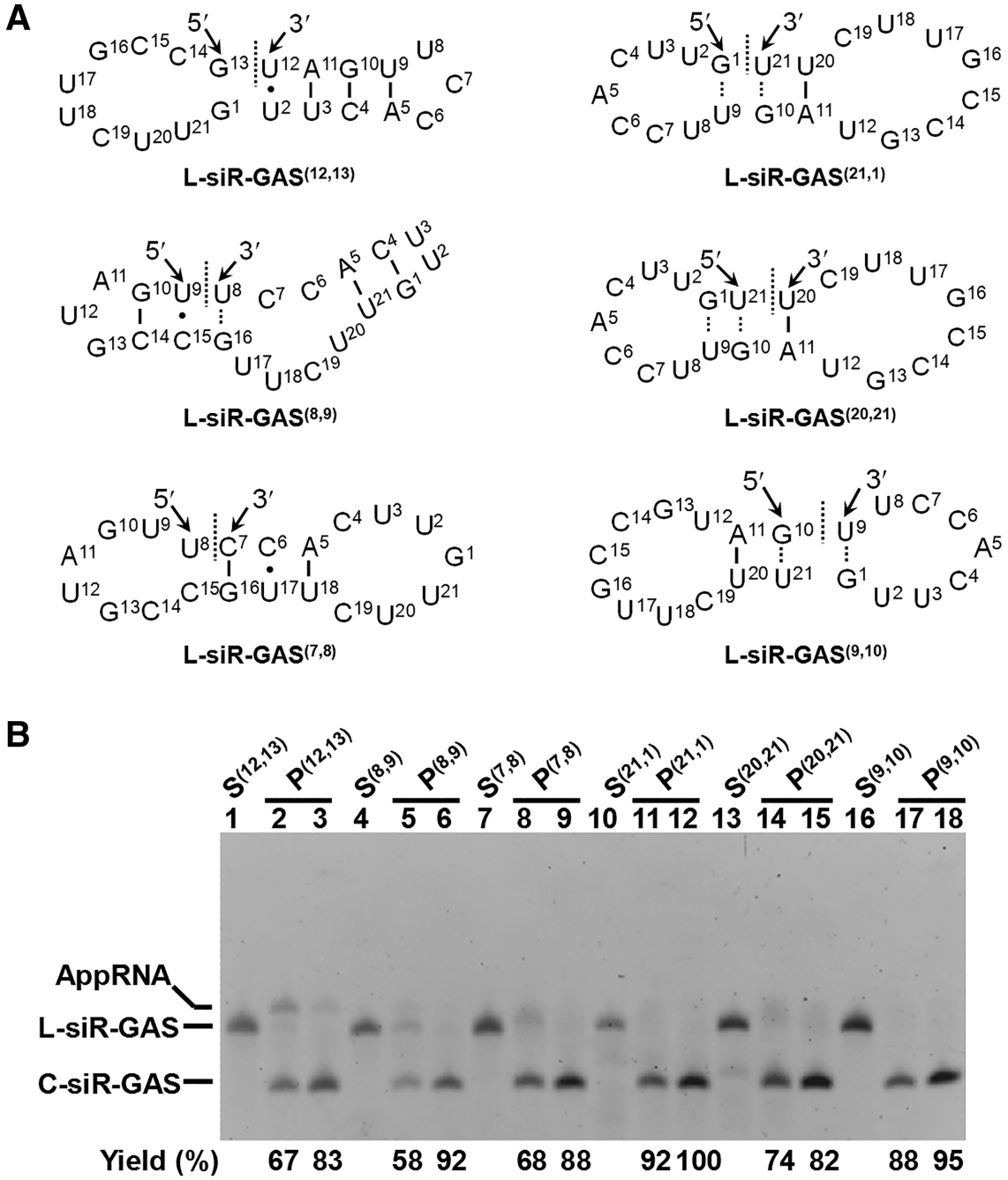

Figure 8. Circularization of L-RNA having smaller number of terminal base pairs. (**A**) Proposed structures of L-siR-GAS$^{(12,13)}$, L-siR-GAS$^{(8,9)}$, L-siR-GAS$^{(7,8)}$, L-siR-GAS$^{(21,1)}$, L-siR-GAS$^{(20,21)}$ and L-siR-GAS$^{(9,10)}$. These structures are some possible structures, which we propose to be formed due to Rnl2 binding for ligation. (**B**) About 12% denaturing PAGE. In lanes 2, 5, 8, 11, 14 and 17, [L-RNA] = 2 μM and [T4 Rnl2] = 0.2 U/μl, 25°C, 2 h, 1 × buffer; in lanes 3, 6, 9, 12, 15 and 18, [L-RNA] = 10 μM and [T4 Rnl2] = 1 U/μl, 12 h, 1 × buffer. Lanes 1, 4, 7, 10, 13 and 16 refer to the substrates alone.

with more base pairs in both terminals. If large amount of C-RNA is required, we can use the substrate with less base pairs, especially in the 5′-phosphate side.

Proposed mechanism for the enormous promotion of circularization by small number of terminal base pairs

It is a great surprise that only very small number of base pairs at the ligation site promote in such an enormous magnitude the intramolecular ligation by Rnl2. We suppose that the enzyme efficiently traps the terminal base pairs which are temporarily formed in the solutions, and this transient specie is eventually converted to stable enzyme–substrate complex. The base pairing in the 3′-OH side should be critically important. Thus, the enzymatic reaction is enormously accelerated by only a few base pairs in the 3′-OH side. Then, the 5′-phosphate group enters the binding pocket of the enzyme, and adenylated through adenylyl transfer from the lysine residue of the enzyme.

The proposed mechanism is further confirmed by the following experiments showing that even smaller number of base pairs is sufficient for circularization under strong reaction conditions, although the reaction rate is relatively slower (Figure 8). Here, C-siR-GAS was cut at various positions other than the best position for 'terminal base-pair strategy'. In L-siR-GAS(7,8), for example, the first and third pairs in the 3′-OH side (C^7-G^{16} and A^5-U^{18}) are matching for circularization, but the second one (C^6-U^{17}) is mismatching. There exists no full match base pair in the 5′-phosphate side. Even under these situations, the circularization by Rnl2 selectively proceeded (lanes 8 and 9). In L-siR-GAS(8,9), only the first pair (U^8-G^{16}) in 3′-OH side is matching for circularization. The 5′-phosphate side is also unstable (only the second pair G^{10}-C^{14} is matching). When this L-RNA was treated by 0.2 U/μl T4 Rnl2 for 2 h, C-siR-GAS was produced in 58% yield (lane 5). Upon the increase of both the amount of Rnl2 and reaction time (1 U/μl for 12 h), the circularization was almost quantitative (lane 6). It is noteworthy that the circularization was successful for all the L-RNA precursors in Figure 8. Accordingly, the decrease in the number of terminal base pairs only decreases the reaction rate, without losing the selective feature. In these examples, at least, only 1 bp in the 3′-OH side is sufficient for circularization. These findings further extend the scope of practical applications of the present 'terminal base-pair strategy'. Even when one cannot find a very good candidate of circularization precursor, the RNA ring is still obtainable simply by increasing the amount of Rnl2 and achieving the reaction for a longer period of time (or other favorable conditions).

It should be noted that these base pairs for L-RNA substrate are not necessarily stable in the absence of Rnl2. During circularization, Rnl2 can help the formation of a nick-like structure (39). For some cases, even when other more stable secondary structures form (circularization cannot occur with these structures, Supplementary Figure S11), the circularization could also be carried out with acceptable efficiency (Figure 8), although these structures slow down the circularization. It has been well accepted that the *in vivo* role of Rnl2 is to repair cleaved RNA, although its detailed mechanism is not clear (37). As shown in this paper, the structure requirements of this enzyme on the substrate are rather small, which could be advantageous for repairing many kinds of RNA damages. Consistently, the structure requirement for nick sealing is also not so strict. Only the 3′-OH side of the nick must be RNA, and both of the 5′-phosphate side of the nick and the template strand can be replaced by DNA (10,30,39).

The present method may be applied to obtain circular ssRNA with various sizes (as shown in Supplementary Figure S13). For example, Daròs *et al*. reported in 2018 that a viroid-derived system was used in *Escherichia coli* to produce large amounts of recombinant RNA for downstream applications (50,51). By using our approach, these long circular RNA may also be produced, because most of these long-stranded RNAs have stable secondary structures (>5 continuous base pairs). By combining these two approaches, many functional RNA may be produced. One of the problems is that long ssRNA of desired sequences with high-purity is difficult to be obtained at present. Development of highly efficient *in vitro* transcription, which can give exact RNA sequences, may solve this problem to some extent.

CONCLUSION

Based on the design of RNA precursor for circularization by T4 Rnl2, highly efficient preparation method of short RNA rings has been established. The secondary structure of targeted RNA ring is first predicted, and the precursor RNA is designed so that a few base pairs are formed at the ligation site. For efficient intramolecular circularization without producing observable polymeric by-products, formation of two or more base pairs in the 3′-OH side of the ligation site, and 0 or 1 bp in the 5′-phosphate side, is preferable. For most of RNAs, appropriate precursor RNA is easily designed by using Mfold or other software (52) for structure prediction (Supplementary Figure S14). Simply by treating this optimized precursor by Rnl2 (without using a splint), the RNA ring is selectively produced. The production of polymeric by-products, which is a critical problem in splint-mediated circularization, is effectively suppressed. Accordingly, various functional RNAs (e.g. siRNA, miRNA and ribozyme) are circularized with high efficiency and high selectivity even at high concentrations (e.g. 50 μM). The selectivity for the formation of RNA ring is further promoted by diluting T4 Rnl2 ligase buffer and also by employing higher reaction temperatures. The present method is useful for large-scale production of RNA rings which are highly potent for medicine, nanotechnology and many other applications. Circularization of longer RNAs is underway in our laboratory to shed light on the roles of functional RNA such as circRNA and riboswitch in cancer, diabetes and other diseases (6).

SUPPLEMENTARY DATA

Supplementary Data are available at NAR Online.

FUNDING

Fundamental Research Funds for Co-construction of Universities in Qingdao [X.L.]; Shandong Provincial Natural Science Foundation, China [ZR2019BC096 to R.A.]; Fundamental Research Funds for the Central Universities [201812009 to M.K.]; National Natural Science Foundation of China [31571937 to X.L.]. Funding for open access charge: Shandong Provincial Natural Science Foundation, China [ZR2019BC096 to R.A.].
Conflict of interest statement. None declared.

REFERENCES

1. Capel,B., Swain,A., Nicolis,S., Hacker,A., Walter,M., Koopman,P., Goodfellow,P. and Lovell-Badge,R. (1993) Circular transcripts of the testis-determining gene Sry in adult mouse testis. *Cell*, **73**, 1019–1030.
2. Ivanov,A., Memczak,S., Wyler,E., Torti,F., Porath,H.T., Orejuela,M.R., Piechotta,M., Levanon,E.Y., Landthaler,M., Dieterich,C. *et al.* (2015) Analysis of intron sequences reveals hallmarks of circular RNA biogenesis in animals. *Cell Rep.*, **10**, 170–177.

3. Jeck,W.R., Sorrentino,J.A., Wang,K., Slevin,M.K., Burd,C.E., Liu,J.Z., Marzluff,W.F. and Sharpless,N.E. (2013) Circular RNAs are abundant, conserved, and associated with ALU repeats. *RNA*, **19**, 141–157.
4. Danan,M., Schwartz,S., Edelheit,S. and Sorek,R. (2011) Transcriptome-wide discovery of circular RNAs in Archaea. *Nucleic Acids Res.*, **40**, 3131–3142.
5. Westholm,J.O., Miura,P., Olson,S., Shenker,S., Joseph,B., Sanfilippo,P., Celniker,S.E., Graveley,B.R. and Lai,E.C. (2014) Genome-wide analysis of drosophila circular RNAs reveals their structural and sequence properties and age-dependent neural accumulation. *Cell Rep.*, **9**, 1966–1980.
6. Kristensen,L.S., Andersen,M.S., Stagsted,L.V.W., Ebbesen,K.K., Hansen,T.B. and Kiems,J. (2019) The biogenesis, biology and characterization of circular RNAs. *Nat. Rev. Genet.*, **20**, 675–691.
7. Memczak,S., Jens,M., Elefsinioti,A., Torti,R., Krueqer,J., Rybak,A., Maier,L., Mackowiak,S.D., Greqersen,L.H., Munschauer,M. *et al.* (2013) Circular RNAs are a large class of animal RNAs with regulatory potency. *Nature*, **495**, 333–338.
8. Salzman,J., Gawad,C., Wang,P.L., Lacayo,N. and Brown,P.O. (2012) Circular RNAs are the predominant transcript isoform from hundreds of human genes in diverse cell types. *PLoS One*, **7**, e30733.
9. Hansen,T.B., Jensen,T.I., Clausen,B.H., Bramsen,J.B., Finsen,B., Damgaard,C.K. and Kjems,J. (2013) Natural RNA circles function as efficient microRNA sponges. *Nature*, **495**, 384–388.
10. Liu,C.X., Li,X., Nan,F., Jiang,S., Gao,X., Xue,W., Cui,Y., Dong,K., Ding,H., Qu,B *et al.*2019) Structure and degradation of circular RNAs regulate PKR activation in innate immunity. *Cell*, **177**, 865–880.
11. Piwecka,M., Glažar,P., Hernandez-Miranda,L.R., Memczak,S., Wolf,S.A., Rybak-Wolf,A., Filipchyk,A., Klironomos,F., Jara,C.A.C., Fenske,P. *et al.* (2017) Loss of a mammalian circular RNA locus causes miRNA deregulation and affects brain function. *Science*, **357**, eaam8526.
12. Chen,C. and Sarnow,P. (1995) Initiation of protein synthesis by the eukaryotic translational apparatus on circular RNAs. *Science*, **268**, 415–417.
13. Müller,S. and Appel,B. (2017) In vitro circularization of RNA. *RNA Biol.*, **14**, 1018–1027.
14. Petkovic,S. and Muller,S. (2015) RNA circularization strategies *in vivo* and *in vitro*. *Nucleic Acids Res.*, **43**, 2454–2465.
15. Wang,L. and Ruffner,D.E. (1998) Oligoribonucleotide circularization by 'template-mediated' ligation with T4 RNA ligase: synthesis of circular hammerhead ribozymes. *Nucleic Acids Res.*, **26**, 2502–2504.
16. Abe,N., Abe,H. and Ito,Y. (2007) Dumbbell-shaped nanocircular RNAs for RNA interference. *J. Am. Chem. Soc.*, **129**, 15108–15109.
17. Abe,N., Abe,H., Nagai,C., Harada,M., Hatakeyama,H., Harashima,H., Ohshiro,T., Nishihara,M., Furukawa,K., Maeda,M. *et al.* (2011) Synthesis, structure, and biological activity of dumbbell-shaped nanocircular RNAs for RNA interference. *Bioconjug. Chem.*, **22**, 2082–2092.
18. Griepenburg,J.C., Ruble,B.K. and Dmochowski,I.J. (2013) Caged oligonucleotides for bidirectional photomodulation of let-7 miRNA in zebrafish embryos. *Bioorg. Med. Chem.*, **21**, 6198–6204.
19. Zhang,L., Liang,D., Wang,Y., Li,D., Zhang,J., Wu,L., Feng,M., Yi,F., Xu,L. and Tang,X. (2018) Caged circular siRNAs for photomodulation of gene expression in cells and mice. *Chem. Sci.*, **9**, 44–51.
20. Zhang,L., Liang,D., Chen,C., Wang,Y., Amu,G., Yang,J., Yu,L., Dmochowski,I.J. and Tang,X. (2017) Circular siRNAs for reducing Off-Target effects and enhancing long-term gene silencing in cells and mice. *Mol. Ther. Nucl. Acids*, **10**, 237–244.
21. Umekage,S. and Kikuchi,Y. (2009) *In vitro* and *in vivo* production and purification of circular RNA aptamer. *J. Biotechnol.*, **139**, 265–272.
22. Holdt,L.M., Kohlmaier,A. and Teupser,D. (2018) Circular RNAs as therapeutic agents and targets. *Front. Physiol.*, **9**, 1262.
23. Litke,J.L. and Jaffrey,S.R. (2019) Highly efficient expression of circular RNA aptamers in cells using autocatalytic transcripts. *Nat. Biotechnol.*, **37**, 667–673.
24. Bohjanen,P.R., Colvin,R.A., Puttaraju,M., Been,M.D. and Garcia-Blanco,M.A. (1996) A small circular TAR RNA decoy specifically inhibits Tat-activated HIV-1 transcription. *Nucleic Acids Res.*, **24**, 3733–3738.
25. Abe,N., Hiroshima,M., Maruyama,H., Nakashima,Y., Nakano,Y., Matsuda,A., Sako,Y., Ito,Y. and Abe,H. (2013) Rolling circle amplification in a prokaryotic translation system using small circular RNA. *Angew. Chem. Int. Ed.*, **52**, 7004–7008.
26. Abe,N., Matsumoto,K., Nishihara,M., Nakano,Y., Shibata,A., Maruyama,H., Shuto,S., Matsuda,A., Yoshida,M. and Abe,H. (2015) Rolling circle translation of circular RNA in living human cells. *Sci. Rep.*, **5**, 16435.
27. Komiyama,M., Yoshimoto,K., Sisido,M. and Ariga,K. (2017) Chemistry can make strict and fuzzy controls for bio-systems: DNA nanoarchitectonics and cell-macromolecular nanoarchitectonics. *Bull. Chem. Soc. Jpn.*, **90**, 967–1004.
28. Komiyama,M., Mori,T. and Ariga,K. (2018) Molecular imprinting: materials nanoarchitectonics with molecular information. *Bull. Chem. Soc. Jpn.*, **91**, 1075–1111.
29. Yin,S., Ho,C.K., Miller,E.S. and Shuman,S. (2004) Characterization of bacteriophage KVP40 and T4 RNA ligase 2. *Virology*, **319**, 141–151.
30. Bullard,D.R. and Bowater,R.P. (2006) Direct comparison of nick-joining activity of the nucleic acid ligases from bacteriophage T4. *Biochem. J.*, **398**, 135–144.
31. Kurschat,W.C., Muller,J., Wombacher,R. and Helm,M. (2005) Optimizing splinted ligation of highly structured small RNAs. *RNA*, **11**, 1909–1914.
32. Gaglione,M., Di Fabio,G. and Messere,A. (2012) Current methods in synthesis of cyclic oligonucleotides and analoga. *Curr. Org. Chem.*, **16**, 1371–1389.
33. Cui,Y., Han,X., An,R., Zhang,Y., Cheng,K., Liang,X. and Komiyama,M. (2018) Terminal hairpin in oligonucleotide dominantly prioritizes intramolecular cyclization by T4 ligase over intermolecular polymerization –An exclusive methodology for producing ssDNA rings. *Nucleic Acids Res.*, **46**, e132.
34. Murakami,T., Sumaoka,J. and Komiyama,M. (2009) Sensitive isothermal detection of nucleic-acid sequence by primer generation–rolling circle amplification. *Nucleic Acids Res.*, **37**, e19.
35. An,R., Li,Q., Fan,Y.Q., Li,J., Pan,X.M., Komiyama,M. and Liang,X.G. (2017) Highly efficient preparation of single-stranded DNA rings by T4 ligase at abnormally low Mg(II) concentration. *Nucleic Acids Res.*, **45**, e139.
36. Kuhn,H. and Frank-Kamenetskii,M.D. (2008) Labeling of unique sequences in double-stranded DNA at sites of vicinal nicks generated by nicking endonucleases. *Nucleic Acids Res.*, **36**, e40.
37. Nandakumar,J., Shuman,S. and Lima,C.D. (2006) RNA ligase structures reveal the basis for RNA specificity and conformational changes that drive ligation forward. *Cell*, **127**, 71–84.
38. Chauleau,M. and Shuman,S. (2013) Kinetic mechanism of nick sealing by T4 RNA ligase 2 and effects of 3′-OH base mispairs and damaged base lesions. *RNA*, **19**, 1840–1847.
39. Cheng,K., An,R., Cui,Y., Zhang,Y., Han,X., Sui,Z., Chen,H., Liang,X. and Komiyama,M. (2019) RNA ligation of very small pseudo nick structures by T4 RNA ligase 2, leading to efficient production of versatile RNA rings. *RSC Adv.*, **9**, 8620–8627.
40. Zuker,M. (2003) Mfold web server for nucleic acid folding and hybridization prediction. *Nucleic Acids Res.*, **31**, 3406–3415.
41. Wang,Z.X., Lu,B.B., Wang,H., Cheng,Z.X. and Yin,Y.M. (2011) MicroRNA-21 modulates chemosensitivity of breast cancer cells to doxorubicin by targeting PTEN. *Arch. Med. Res.*, **42**, 281–290.
42. Bi,F., Fan,D., Hui,H., Wang,C. and Zhang,X. (2001) Reversion of the malignant phenotype of gastric cancer cell SGC7901 by c-erbB-2–specific hammerhead ribozyme. *Cancer Gene Ther.*, **8**, 835–842.
43. Liang,X., Zhou,M., Kato,K. and Asanuma,H. (2013) Photoswitch nucleic acid catalytic activity by regulating topological structure with a universal supraphotoswitch. *ACS Synth. Biol.*, **2**, 194–202.
44. Chen,G. and Turner,D.H. (2006) Consecutive GA pairs stabilize medium-size RNA internal loops. *Biochemistry*, **45**, 4025–4043.
45. Walter,A.E. and Turner,D.H. (1994) Sequence dependence of stability for coaxial stacking of RNA helixes with Watson-Crick base paired interfaces. *Biochemistry*, **33**, 12715–12719.
46. Yu,L., Liang,D., Chen,C. and Tang,X. (2018) Caged siRNAs with single cRGD modification for photoregulation of exogenous and endogenous gene expression in cells and mice. *Biomacromolecules.*, **19**, 2526–2534.

47. Ho,C.K., Wang,L.K., Lima,C.D. and Shuman,S. (2004) Structure and mechanism of RNA ligase. *Structure*, **12**, 327–339.
48. Yuan,C., Lou,X.W., Rhoades,E., Chen,H. and Archer,L.A. (2007) T4 DNA ligase is more than an effective trap of cyclized dsDNA. *Nucleic Acids Res.*, **35**, 5294–5302.
49. Rossi,R., Montecucco,A., Ciarrocchi,G. and Biamonti,G. (1997) Functional characterization of the T4 DNA ligase: a new insight into the mechanism of action. *Nucleic Acids Res.*, **25**, 2106–2113.
50. Daròs,J.A., Aragonés,V. and Cordero,T. (2018) A viroid-derived system to produce large amounts of recombinant RNA in *Escherichia coli*. *Sci. Rep.*, **8**, 1904.
51. Cordero,T., Aragonés,V. and Daròs,J.A. (2018) Large-scale production of recombinant RNAs on a circular scaffold using a viroid-derived system in *Escherichia coli*. *JOVE*, **141**, e58472.
52. Reuter,J.S. and Mathews,D.H. (2010) RNAstructure: software for RNA secondary structure prediction and analysis. *BMC Bioinformatics*, **11**, 129.